Molecular imaging of the human pulmonary vascular endothelium using an adrenomedullin receptor ligand.

François Harel, Xavier Levac, Quang T Nguyen, Myriam Létourneau, Sophie Marcil, Vincent Finnerty, Marième Cossette, Alain Fournier, Jocelyn Dupuis

RESEARCH ARTICLE

Molecular Imaging of the Human Pulmonary Vascular Endothelium Using an Adrenomedullin Receptor Ligand

François Harel, Xavier Levac, Quang T. Nguyen, Myriam Létourneau, Sophie Marcil, Vincent Finnerty, Mariève Cossette, Alain Fournier, and Jocelyn Dupuis

Abstract

This phase I study (NCT01539889) evaluated the safety, efficacy, and dosing of PulmoBind for molecular imaging of pulmonary circulation. PulmoBind is a ligand of the adrenomedullin receptor abundantly distributed in lung capillaries. Labeled with ^{99m}Tc, it allows single-photon emission computed tomographic (SPECT) imaging of lung perfusion. In preclinical studies, PulmoBind scans enabled detection of lung perfusion defects and quantification of microcirculatory occlusion caused by pulmonary hypertension. Healthy humans ($N = 20$) were included into escalating groups of 5 mCi ($n = 5$), 10 mCi ($n = 5$), or 15 mCi ($n = 10$) ^{99m}Tc-PulmoBind. SPECT imaging was serially performed, and ^{99m}Tc-PulmoBind dosimetric analysis was accomplished. The radiochemical purity of ^{99m}Tc-PulmoBind was greater than 95%. There were no safety concerns at the three dosages studied. Imaging revealed predominant and prolonged lung uptake with a mean peak extraction of 58% ± 7%. PulmoBind was well tolerated, with no clinically significant adverse event related to the study drug. The highest dose of 15 mCi provided a favorable dosimetric profile and excellent imaging. The postural lung perfusion gradient was detectable. ^{99m}Tc-PulmoBind is safe and provides good quality lung perfusion imaging. The safety/efficacy of this agent can be tested in disorders of pulmonary circulation such as pulmonary arterial hypertension.

CURRENTLY, only one agent is approved in nuclear medicine to study lung circulation: macroaggregates of albumin labeled with ^{99m}Tc (^{99m}Tc-MAA). ^{99m}Tc-MAA is used almost exclusively to detect large pulmonary perfusion defects caused by embolism. Since this agent is larger than small pulmonary vessels, after injection, it is physically trapped, which enables external detection. The potential limitations of ^{99m}Tc-MAA therefore include the inability to image the small pulmonary circulation beyond the point of obstruction, limiting its sensitivity to detect small vascular defects such as those caused by pulmonary arterial hypertension, as well as potential infectious risks because this agent is derived from human albumin. Another limitation is that approximately 350,000 particles of this tracer are injected and block as many pulmonary vessels in the process. This undesirable ''physical'' blockage of pulmonary circulation in subjects with an already compromised pulmonary circulation represents a current warning on the product monograph. Furthermore, the product may be allergenic in subjects sensitive to albumin and presents supply issues as it is derived from human albumin. Replacement agents that would provide functional assessment of lung perfusion without these caveats are desirable. Molecular imaging agents targeting the pulmonary vascular endothelium have been evaluated for this purpose.[1]

Adrenomedullin is a 52–amino acid multifunctional regulatory peptide expressed in a wide range of tissues, including the lungs.[2–4] Its specific heterodimeric receptor is composed of the calcitonin-like receptor (CLR) and the receptor activity–modifying protein 2 or 3 (RAMP2, RAMP3).[5] The receptor is abundantly expressed in human alveolar capillaries and mostly distributed at the surface of the endothelium.[6–8] Accordingly, the lungs contain adrenomedullin binding sites at a density higher than that for any other organ studied[8,9] and are a primary site for adrenomedullin clearance.[10,11] We hypothesized that radiolabeled adrenomedullin derivatives could be used as tracers to evaluate the integrity of pulmonary circulation. Through

Presented at the Sixth Annual Scientific Workshops and Debates of the Pulmonary Vascular Institute, Istanbul, January 24, 2013. An abstract was published in Pulmonary Circulation 2013;3:706.

From the Research Center, Montreal Heart Institute, and the Departments of Nuclear Medicine and Medicine, Université de Montréal, Montreal, QC; Montreal Heart Institute Coordinating Center, Montreal, QC; and INRS-Institut Armand-Frappier, Laval, QC.

Address reprint requests to: Jocelyn Dupuis, MD, PhD, FRCP, FACC, Research Center, Montreal Heart Institute, 5000 Belanger Street, Montreal, QC H1T 1C8; e-mail: dupuisj@me.com.

DOI 10.2310/7290.2015.00003

DECKER

rational design and structure-activity studies, we developed various derivatives[12] that would maintain binding affinity without significant biologic effects while enabling the addition of a chelating moiety for a suitable radioisotope.[13] These derivatives demonstrated good-quality lung imaging, enabling the detection of large perfusion defects mimicking pulmonary embolism,[14] but also microcirculatory occlusion in a model of pulmonary arterial hypertension.[15] A lead compound possessing the desired properties was developed,[13] called PulmoBind. This phase I trial tested the safety and efficacy of PulmoBind.

Materials and Methods

The trial was conducted at the Montreal Heart Institute and registered at ClinicalTrials.gov (NCT01539889). The study was approved by the Ethics Committee (No. CER 08-1062) and conducted in accordance with the amended Declaration of Helsinki. All participants signed a written informed consent form.

PulmoBind synthesis was performed as previously described.[13] The Fmoc- (polyethylene glycol)4-COOH used as a spacer in the peptide synthesis was purchased from Quanta Biodesign Ltd. Disulfide bond formation to yield a cyclic derivative was performed by overnight air oxidation after dissolution of the linear peptide in an aqueous solution (pH 8.8) at a concentration of 0.1 mg/mL. The peptide was purified by reversed-phase high-performance liquid chromatography (RP-HPLC). The amino acid sequence of PulmoBind, in comparison with that of native human adrenomedullin (hAM), is shown in Figure S1 (online version only). The purity of the final product was evaluated by analytical RP-HPLC ($>$ 98%), and matrix-assisted laser desorption ionization–time-of-flight mass spectrometry (MALDI-ToF MS; Voyager DE, Applied Biosystems) was used to confirm the right mass of the synthetic product (m/z_{theo}: 4270.82; m/z_{obs}: 4271.71).

Unidose vials were prepared containing 18.5 μg of lyophilized PulmoBind. The labeling procedure was performed by the addition of 20 μL acetate buffer (1 M, pH 5.5), 200 μL Na_3PO_4 (0.1 M, pH 12), 31.25 μL $SnCl_2$ (0.8 mg/mL in HCl 0.05M), and 30 mCi of $Na^{99m}TcO_4$ (28.9 pmol). Finally, 1 mL of NaH_2PO_4 (0.1 M, pH 4.5) was added to adjust the pH to 7.4. ^{99m}Tc-PulmoBind was purified using a C_{18} Sep-Pak cartridge, and radiochemical purity was tested by instant thin-layer chromatography. Radiometric and ultraviolet (UV) HPLC chromatograms of the final drug product are shown in Figure S2 (online version only). It appears that the radiolabeled product exists as one product, but due to the very small quantity of starting drug substance, the labeled product generated through this protocol is undetectable by a UV detector. Specific activity is estimated to be around 6.8 mCi/mmol, and the average radiochemical yield was 53.6% $\pm$ 4.5%.

There were three study objectives: safety, efficacy and dosing. A safety objective aimed to determine pharmacokinetics and biodistribution to perform dosimetric evaluation; another safety objective was to evaluate any effect on vital signs and on hematology and biochemistry profiles and to evaluate any local or systemic reactions. The efficacy objective was to evaluate the ability of PulmoBind to allow lung perfusion imaging in human. The third objective determined the optimal dose by evaluating the safety/efficacy in three groups with escalating dosages.

Study Design and Safety Assessments

Twenty healthy subjects were recruited. Detailed inclusion and exclusion criteria are discussed in the Supplementary Material (online version only).

The study timeline is shown in Figure S3 (online version only). Study subjects were divided into three groups receiving increasing intravenous dosages of ^{99m}Tc-PulmoBind: group A, 5 mCi (185 MBq, $n = 5$); group B, 10 mCi (370 MBq, $n = 5$); and group C, 15 mCi (555 MBq, $n = 10$). Study procedures were performed according to Figure 1. All adverse events occurring during the study were reported and characterized.

Dosimetry calculations were performed as follows. A transmission scan was performed to obtain an attenuation map using a cobalt-57 flood source. Whole body scans were then obtained serially after injection (see Figure 1) with a dual-head e-cam (Siemens Medical Systems) using a low-energy high-resolution collimator with 256 $\times$ 1,024 matrices. Acquisitions were evaluated with *MATLAB* version 7.01 (MathWorks, Natick, MA). Regions of interest were drawn over the most visible organs from anterior and posterior projections. Background noise was removed from each organ's region of interest. The geometric mean of anterior and posterior view images was used to calculate the estimated ^{99m}Tc total count and mean counts dose, in counts per minute, for the organ.

A regression model (double exponential or gamma variate depending on the organ) was applied. Collected urine and stool values were added to the biodistribution calculation for the bladder and intestines, respectively, to model a closed system. Activity in the rest of the body or residual cumulative dose was estimated to be the

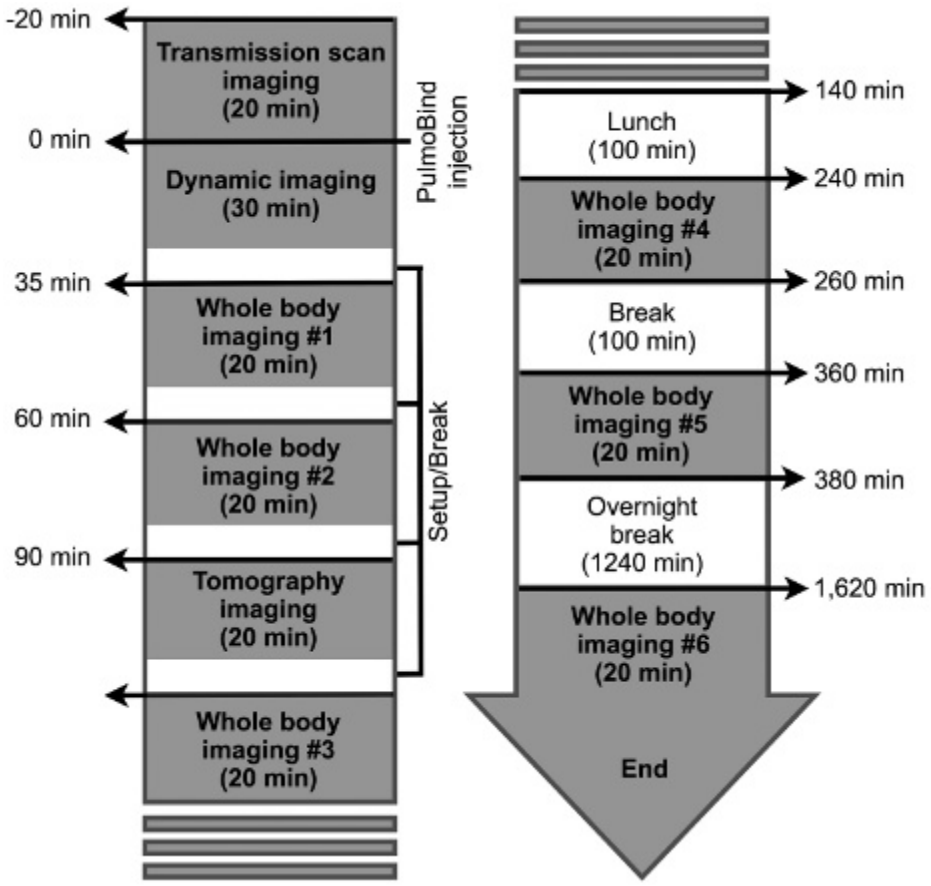

Figure 1. Nuclear medicine imaging protocol.

theoretical total cumulative dose for ^{99m}Tc less the cumulative dose of all the other organs. The final cumulative dose for the bladder was recalculated using *OLINDA/EXM* 1.0 software (Organ Level Internal Dose Assessment Code) with the voiding bladder model using a voiding interval of 2 and 4.8 hours. Percentage of the total dose in the feces was used to calculate the cumulative doses of the different parts of the digestive system with the International Commission on Radiological Protection gastrointestinal model provided in *OLINDA/EXM* software. The dose to the ovaries was estimated from biodistribution measured in males but applied to a female model.

Blood samples (6 mL) were obtained to determine plasma kinetics of PulmoBind using a two-phase exponential-decay equation with GraphPad *Prism* version 6.0 software (GraphPad Software, La Jolla, CA).

For precise quantification of pulmonary clearance of PulmoBind, we performed a dynamic acquisition of the chest for 20 minutes following injection (see Figure 1) coupled with whole body images later in time.

Lung imaging quality was determined by two nuclear medicine specialists from whole body image acquisitions. They graded the scans from I (mediocre) to IV (superior quality). Quality was judged in relation to that usually achieved with radiolabeled albumin macroaggregate lung perfusion scans based on the investigator's judgment.

Statistical Analysis

Analysis was performed for the three study groups combined and for each separately. Sample size estimation was based on blood pressure variation. Blood pressure measured in 1,743 Canadian individuals was 121 ± 16 mm Hg (mean ± SD) for systolic and 78 ± 11 mm Hg for diastolic.[16] Based on these values and assuming a pre-/postsystolic blood pressure correlation of 0.5, a sample size of 20 (whole study group) allowed the detection of a reduction of 12 mm Hg in systolic blood pressure (−10%) with a power of 90% and an alpha of 0.05. For a sample size of 10 (group C, 15 mCi), the power to detect a reduction of

18 mm Hg (−15%) was 90%. For a sample size of 5 (group A, 5 mCi, and group B, 10 mCi), the power to detect a reduction of 24 mm Hg (−20%) was 80%.

Statistical analysis was performed using *SAS* version 9.2 (SAS Institute, Cary, NC). The maximum reduction in vital signs from visit 1 (preinjection) to 360 minutes was analyzed using an analysis of variance (ANOVA) model with study group as the main factor. Under this model, the mean maximum reduction in the three study groups combined and in each group separately was estimated and presented with a 95% confidence interval (CI). In addition, vital signs at day 1 (preinjection), 1 minute, 2 minutes, 3 minutes (during injection), 5 minutes, 15 minutes, 30 minutes, 1 hour, 2 hours, 3 hours, 4 hours, 5 hours, and 6 hours were analyzed using a repeated measures ANOVA model including study group, time, and study group × time interaction as the main factors. Under this model, differences from day 1 (preinjection) to each follow-up time point were estimated and presented with a 95% CI. Oral temperature, hematology, and biochemistry parameters were analyzed using a repeated measures ANOVA model including study group, time, and study group × time interaction as the main factors. The focus of these analyses is on showing that the bounds of the 95% CI of the change over time and maximum reduction are within acceptable limits. Due to too low power and the small sample size, adverse events, categorical safety parameters, and the efficacy end point of lung perfusion are simply tabulated. Values are reported as mean ± SD or as mean (95% CI).

Results

Two women and 18 men were recruited. The mean age was 33 ± 14 years (range 20–71 years), and the mean weight was 75 ± 14 kg. The mean drug substance purity by HPLC analysis and MALDI-ToF MS was > 98%. The radiochemical purity of ^{99m}Tc-PulmoBind was 95 ± 4%. All subjects were included into the safety analysis. In one subject, the injected ^{99m}Tc-PulmoBind showed prolonged forearm vein retention due to an anomalous venous return (nonconnecting veins). This subject was therefore not included in the plasma kinetic and biodistribution analysis.

Plasma kinetics of PulmoBind is shown in Figure 2. Plasma levels rapidly decreased with a distribution half-life of 6 minutes (95% CI 4–12) and an elimination half-life of 90 minutes (95% CI 65–149).

Biodistribution was analyzed for the whole study group (n = 19). ^{99m}Tc-PulmoBind was rapidly retained by the lungs, with a peak uptake of 58% ± 7% ID occurring 5.5 ± 0.7 minutes following injection. Lung activity cleared very slowly, with 44% ± 6% ID after 35 minutes and 33% ± 5% ID after 60 minutes. Whole body imaging in anterior and posterior views with the lung activity-time curve of a study subject is shown in Figure 3. A video demonstrating dynamic ^{99m}Tc-PulmoBind lung uptake and body biodistribution over 6 hours is provided in the online version (Video S1).

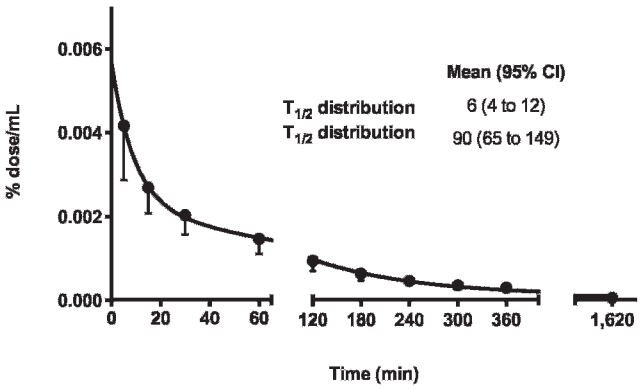

Figure 2. Plasma kinetics of ^{99m}Tc-PulmoBind in humans.

Organs biodistribution is shown in Figure 4. The majority of the tracer is retained by the lungs, followed in intensity by the kidneys and the liver. Increased urinary, gallbladder, and bowel activity with time confirms these routes of elimination. Tomographic imaging at 90 minutes is shown in Figure 5. There is still substantial lung activity, and, interestingly, higher activity is evident in the more gravity-dependent (dorsal) regions. A 360° animation is shown in Video S2 (online version only).

Safety Parameters and Imaging Quality

Sample size was estimated to detect a variation of 12 mm Hg for the whole study group (N = 20), 24 mm Hg in the 5 mCi and 10 mCi groups (n = 5), and 18 mm Hg in the 15 mCi group (n = 10). These values are also deemed clinically significant.

For the 20 subjects, the maximum reduction in blood pressure (mm Hg) for day 1, from preinjection to 6 hours, is −7.4 (−10.3, −4.4) (mean with 95% CI) for systolic blood pressure and −9.8 (−13.4, −6.2) for diastolic blood pressure. Mean systolic and diastolic blood pressures measured throughout the study for the 20 subjects are presented in Figure 6. The change in systolic and diastolic pressures compared to preinjection values is also depicted. The dotted lines represent a 12 mm Hg variation,

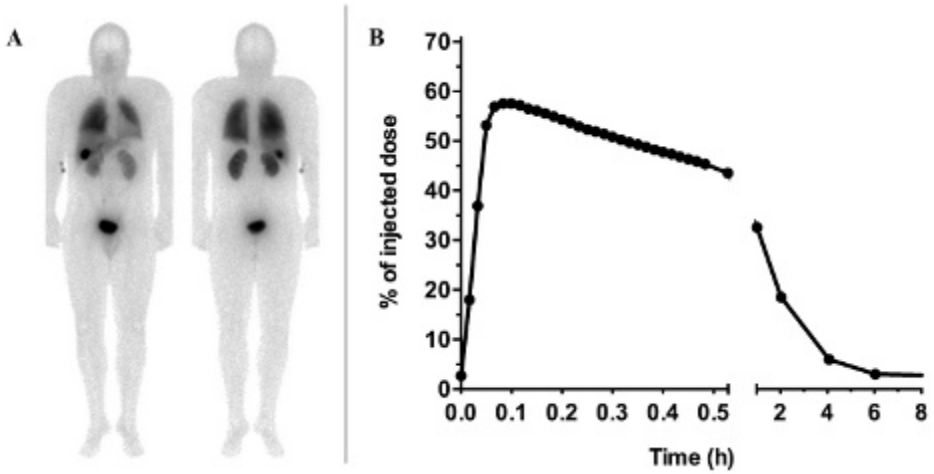

Figure 3. Whole body planar SPECT imaging in a human (subject 006) 60 minutes after injection of ^{99m}Tc-PulmoBind (A) and activity-time curve for the lung activity of the tracer (B).

considered to be clinically significant. Table 1 shows the maximum reduction in systolic and diastolic blood pressure (irrespective of its time point) and the confidence interval for each study group. There were no clinically significant changes. Similarly, there were no significant variations in heart rate, respiratory rate, oxygen saturation, and body temperature (data not shown). Biochemistry and hematology laboratories remained within the normal clinical range.

Activity-time curves for subjects receiving the nominal dose of 15 mCi of ^{99m}Tc-PulmoBind are presented in Figure 4B. About 97% of the cumulative dose can be predicted from the organ modeling. The radiation doses absorbed by target organs and the total body are shown in Table 2.

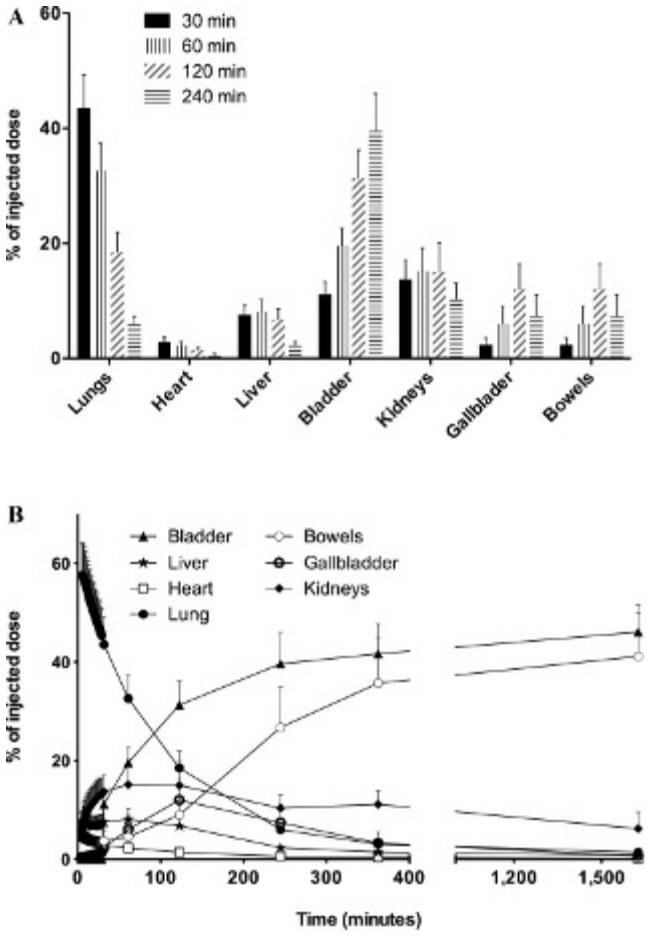

Figure 4. *A*, Organ biodistribution of ^{99m}Tc-PulmoBind at various time points after injection for all study groups combined ($n = 19$). *B*, Activity-time curves in the organs of nine subjects receiving 15 mCi (555 MBq) of ^{99m}Tc-PulmoBind. Values are mean ± SD.

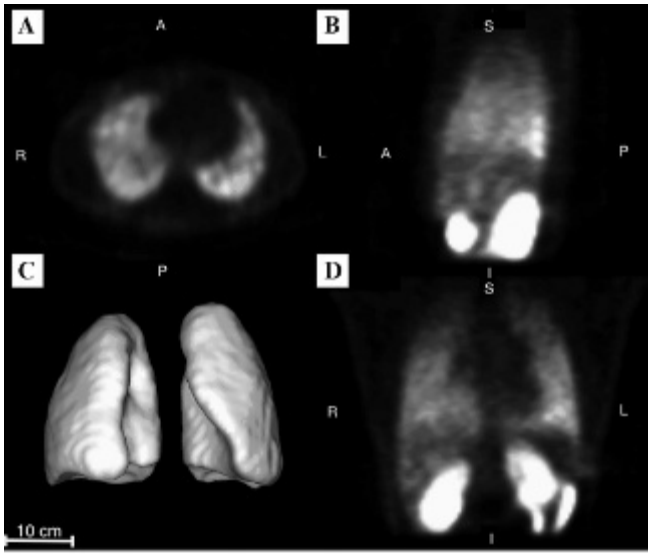

Figure 5. Tomographic SPECT imaging of the lungs 90 minutes after ^{99m}Tc-PulmoBind injection in a human in transversal (A), sagittal (B), and frontal (D) views. There is greater activity in the gravity-dependent (dorsal) region of the lungs. Three-dimensional reconstruction is shown in *C*.

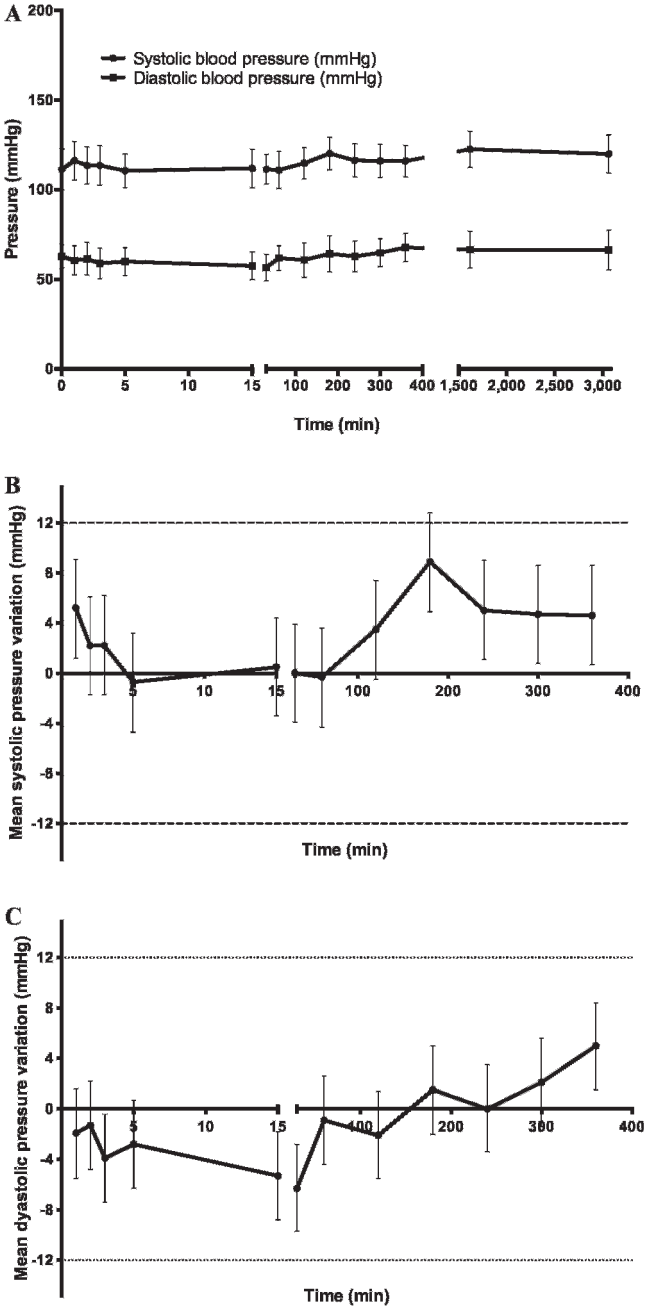

Figure 6. Effect of PulmoBind on systemic blood pressure of all study groups ($N = 20$). The graph *A* represents mean systolic and diastolic blood pressures. Variation of systolic (*B*) and diastolic (*C*) blood pressure compared to preinjection values. The *dotted lines* represent a 12 mm Hg difference predetermined to be clinically significant.

There were no serious adverse events. The frequency, relationship to the study drug, and intensity of nonserious events are shown in Figure S4 (online version only). There were no events definitely related to the study drug. There was one nonserious event probably related to the study drug as a subject experienced mild pain at the injection site.

Imaging quality is shown in Figure 7. At the dosage of 15 mCi (555 MBq), a substantial proportion of subject showed superior quality at both 35 minutes (60%) and 60 minutes (30%) following injection.

Discussion

PulmoBind was developed through rational design and structure-activity studies to specifically and safely image pulmonary circulation by binding to the adrenomedullin receptor.[13] Adrenomedullin is a 52–amino acid peptide possessing various biologic effects, among them vasodilation. Adrenomedullin may be involved in pulmonary hypertension, and its chronic administration in animal models resulted in therapeutic improvement.[17] The lung is a primary site for plasma adrenomedullin clearance[10] and displays a high density of receptors, mostly in alveolar capillaries.[6] Using labeled derivatives, we demonstrated specific and important lung uptake after intravenous injection.[12] Furthermore, we demonstrated that labeled adrenomedullin derivatives could image large lung perfusion defects mimicking pulmonary embolism as well as small pulmonary vessel obliteration in the monocrotaline model of pulmonary arterial hypertension.[14,15] In the latter, there is also reduced pulmonary expression of the receptor. Although human pathologic data demonstrated important distribution of adrenomedullin binding sites in the capillaries, this is the first in vivo demonstration that the human lung represents a primary site for circulating adrenomedullin clearance. The lung uptake is prolonged, suggesting that the tracer may irreversibly bind to its receptor to be later internalized. Previous data in dogs were also suggestive because there was no detectable return of ligand within a pulmonary transit time.[14] The current study therefore validates the adrenomedullin receptor as an appealing target to noninvasively probe the integrity of pulmonary circulation in humans.

The maximal dose of ^{99m}Tc-PulmoBind used in the current study (15 mCi) contained a maximum of 18.5 μg of peptide. This dosage did not cause any clinically significant hemodynamic effect. There were no variations in blood pressure outside the predetermined clinically significant range. The structure of PulmoBind was indeed designed to reduce any potential hypotensive effects observed with adrenomedullin by substituting the four key amino acid residues Arg^{17}-Phe^{18}-Gly^{19}-Thr^{20} contained within the cystine structure (S – S bridged Cys^{16} and Cys^{21}) with a four-unit polyethylene glycol spacer.

Table 1. Mean Maximum Reduction per Study Group for Systolic and Diastolic Pressures

Blood Pressure (mm Hg)	*Group*	*Maximum Reduction*	*95% CI*
Systolic	5 mCi*	−17.2	−23.0, −11.4
	10 mCi†	−3.6	−9.4, 2.2
	15 mCi‡	−4.3	−8.4, −0.2
Diastolic	5 mCi*	−11.4	−18.7, −4.1
	10 mCi†	−7.8	−15.1, −0.5
	15 mCi‡	−10	−15.1, −4.9

*185 MBq.
†370 MBq.
‡555 MBq.

The dosimetry for patients selected for the nominal dose of 15 mCi ^{99m}Tc-PulmoBind reveals an effective dose of approximately 6 to 8 mSv. The liver and the kidneys rapidly eliminate the activity. By comparison, the absorbed dose is similar to single-photon emission computed tomographic (SPECT) myocardial scintigraphy, a commonly used diagnostic test. At the dosage of 15 mCi, ^{99m}Tc-PulmoBind provided lung scans that were judged to be of superior quality compared to what is generally obtained with labeled albumin macroaggregates. For an average adult of 70 kg, a dose of 4 mCi of ^{99m}Tc-MAA results in a lower estimated whole body absorbed dose of 0.6 mSv, whereas the absorbed dose to the lungs is similar to that of PulmoBind at 8.8 mSv (Draximage MAA kit monography, Jubilant Draximage, Quebec). At our institution, we usually inject about 10 mCi of ^{99m}Tc-MAA to perform a lung scan.

Table 2. Absorbed Radiation after ^{99m}Tc-PulmoBind

Target Organ	*Equivalent Dose (mSv/555 mBq)*
Gallbladder	25.25
Kidneys	23.60
Lungs	8.01
Liver	3.97
Spleen	2.37
Bladder	
2.0-hour void	12.08
4.8-hour void	28.29
Testicles	
2.0-hour void	0.58
4.8-hour void	1.02
Ovaries*	
2.0-hour void	6.60
4.8-hour void	7.48
	Effective Dose (mSv/555 mBq)
Total body	
Man 2.0-hour void	5.58
Man 4.8-hour void	6.45
Woman 2.0-hour void	6.81
Woman 4.8-hour void	7.68

*Dose to the ovaries is estimated from male biodistribution, applied to a female dosimetry model.

Albumin macroaggregate injections are composed of particles generally varying in size from 10 to 70 μm. The number of particles injected varies but is generally around 350,000 per injection. These particles will therefore block alveolar capillaries but also larger precapillary vessels. By contrast, ^{99m}Tc-PulmoBind does not block vessels but binds to the vascular endothelial cells expressing its receptors. Since the greatest vascular surface area resides in the alveolar capillaries, where intense adrenomedullin binding has previously been observed in human lungs,[6] use of the molecular agent PulmoBind may provide superior imaging. Interestingly, the normal dorsoventral postural perfusion gradient was also easily detectable, demonstrating that PulmoBind distributes according to blood flow.

Numerous disorders can affect the physical and biologic integrity of pulmonary circulation. Unfortunately, there is currently no noninvasive method to directly probe the status of pulmonary circulation. The pulmonary capillaries represent a very large metabolically active vascular surface area. Future trials are necessary to determine if clinical conditions that affect the distribution, density, and/or activity of the adrenomedullin receptor may be evaluated using PulmoBind. More specifically, PulmoBind could be evaluated as a noninvasive test to image pulmonary arterial hypertension, a condition associated with endothelial dysfunction and loss of pulmonary microcirculation.

Conclusion

This phase I study assessed the safety and efficacy of PulmoBind, a novel lung molecular imaging agent

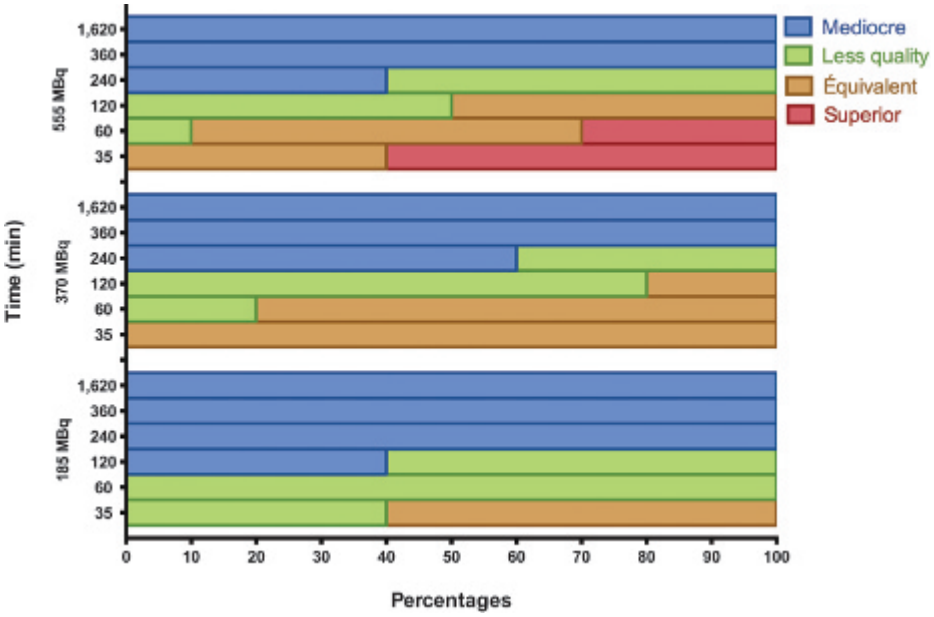

Figure 7. Imaging quality at dosages of 5 mCi (185 MBq, $n = 5$), 10 mCi (370 MBq, $n = 5$), and 15 mCi (555 MBq, $n = 9$) of ^{99m}Tc-PulmoBind at various time points after injection.

designed to noninvasively evaluate pulmonary circulation. In this first-in-human trial, there were no safety concerns, and PulmoBind provided very good-quality lung imaging. This novel molecular imaging agent should now be tested in disorders of pulmonary circulation.

Acknowledgments

We would like to thank Emma Dedelis and Hubert Poiffaut for their technical assistance and Luc Harvey and Lucette Whittom for their help with the study protocol and case report forms.

Financial disclosure of authors: This work was supported by the Quebec Consortium for Drug Discovery. Dr. Dupuis is a shareholder of PulmoScience Inc., a company that holds commercial rights to PulmoBind. The other authors report no conflicts.

Financial disclosure of reviewers: None reported.

References

1. Dupuis J, Harel F, Nguyen QT. Molecular imaging of the pulmonary circulation in health and disease. Clin Transl Imaging 2014;2:415–26, doi:10.1007/s40336-014-0076-9.
2. Asada Y, Hara S, Marutsuka K, et al. Novel distribution of adrenomedullin-immunoreactive cells in human tissues. Histochem Cell Biol 1999;112:185–91, doi:10.1007/s004180050406.
3. Hwang IS, Tang F. Peripheral distribution and gene expression of adrenomedullin in the rat: possible source of blood adrenomedullin. Neuropeptides 2000;34:32–7, doi:10.1054/npep.1999.0783.
4. Kitamura K, Sakata J, Kangawa K, et al. Cloning and characterization of cDNA encoding a precursor for human adrenomedullin. Biochem Biophys Res Commun 1993;194:720–5, doi:10.1006/bbrc.1993.1881.
5. Conner AC, Simms J, Hay DL, et al. Heterodimers and family-B GPCRs: RAMPs, CGRP and adrenomedullin. Biochem Soc Trans 2004;32:843–6, doi:10.1042/BST0320843.
6. Hagner S, Haberberger R, Hay DL, et al. Immunohistochemical detection of the calcitonin receptor-like receptor protein in the microvasculature of rat endothelium. Eur J Pharmacol 2003;481:147–51.
7. Hagner S, Stahl U, Knoblauch B, et al. Calcitonin receptor-like receptor: identification and distribution in human peripheral tissues. Cell Tissue Res 2002;310:41–50, doi:10.1007/s00441-002-0616-x.
8. Martinez A, Miller MJ, Catt KJ, Cuttitta F. Adrenomedullin receptor expression in human lung and in pulmonary tumors. J Histochem Cytochem 1997;45:159–64, doi:10.1177/002215549704500202.
9. Owji AA, Smith DM, Coppock HA, et al. An abundant and specific binding site for the novel vasodilator adrenomedullin in the rat. Endocrinology 1995;136:2127–34.
10. Dupuis J, Caron A, Ruel N. Biodistribution, plasma kinetics and quantification of single-pass pulmonary clearance of adrenomedullin. Clin Sci (Lond) 2005;109:97–102, doi:10.1042/CS20040357.
11. Dschietzig T, Azad HA, Asswad L, et al. The adrenomedullin receptor acts as clearance receptor in pulmonary circulation. Biochem Biophys Res Commun 2002;294:315–8, doi:10.1016/S0006-291X(02)00474-6.
12. Fu Y, Letourneau M, Nguyen QT, et al. Characterization of the adrenomedullin receptor acting as the target of a new radiopharmaceutical biomolecule for lung imaging. Eur J Pharmacol 2009;617:118–23.
13. Létourneau M, Nguyen QT, Harel F, et al. PulmoBind, an adrenomedulin-based molecular lung imaging tool. J Nucl Med 2013;54:1789–96.

14. Harel F, Fu Y, Nguyen QT, et al. Use of adrenomedullin derivatives for molecular imaging of pulmonary circulation. J Nucl Med 2008;49:1869–74, doi:10.2967/jnumed.108.054023.
15. Dupuis J, Harel F, Fu Y, et al. Molecular imaging of monocrotaline-induced pulmonary vascular disease with radiolabeled linear adrenomedullin. J Nucl Med 2009;50:1110–5.
16. Wolf HK, Tuomilehto J, Kuulasmaa K, et al. Blood pressure levels in the 41 populations of the WHO MONICA project. J Hum Hypertens 1997;1:733–42, doi:10.1038/sj.jhh.1000531.
17. Yoshihara F, Nishikimi T, Horio T, et al. Chronic infusion of adrenomedullin reduces pulmonary hypertension and lessens right ventricular hypertrophy in rats administered monocrotaline. Eur J Pharmacol 1998;355:33–9.

Molecular Imaging of the Human Pulmonary Vascular Endothelium Using an Adrenomedullin Receptor Ligand

François Harel, Xavier Levac, Quang T. Nguyen, Myriam Létourneau, Sophie Marcil, Vincent Finnerty, Marième Cossette, Alain Fournier, and Jocelyn Dupuis

Supplementary Material

Inclusion Criteria

1. Male and female subjects greater than 18 years of age. Female subjects must be postmenopausal (defined as 2 years after the last menstrual cycle).
2. Baseline measurements must be in the limit of normal for the following:
   a. Blood pressure: systolic 100 to 140 mm Hg, and diastolic 50 to 90 mm Hg
   b. Heart rate: 60 to 100 beats per minute
   c. Oral temperature: $< 37.6^{\circ}C$
   d. Respiratory rate: 12 to 20 breaths per min
   e. Lung function tests
   f. Echocardiogram, including estimation of pulmonary artery systolic pressure
   g. Chest radiograph
   h. Electrocardiogram

Exclusion Criteria

1. Any known chronic or acute medical condition with or without the need for chronic pharmacologic therapy or any condition that may interfere with normal biodistribution of DFH-12. This includes but is not restricted to lung parenchymal or lung vascular diseases such as chronic obstructive pulmonary disease, bronchitis, lung cancer, pleural effusion, emphysema, asthma, pulmonary fibrosis, occupational lung disease, pulmonary hypertension (primary or secondary), systemic hypertension, diabetes, cancer, kidney disease, liver disease, heart failure or previous myocardial infarction, coronary artery disease, peripheral vascular disease, or inflammatory disease.
2. Subjects requiring chronic administration of any substance for a medical condition
3. Active smoking or history of smoking for more than 1 year in the past 10 years
4. Known self-reported alcoholism (active or abstinent). Subjects with possible alcohol dependence will complete the Michigan Alcohol Screening Test (MAST) and will be excluded if the score is ≥ 6.
5. Unable to tolerate study procedures (e.g., venipuncture, movement restrictions during imaging)
6. Previous nuclear study since 1 week (to avoid cross-contamination)

Presented at the Sixth Annual Scientific Workshops and Debates of the Pulmonary Vascular Institute, Istanbul, January 24, 2013. An abstract was published in Pulmonary Circulation 2013;3:706

From the Research Center, Montreal Heart Institute, and the Departments of Nuclear Medicine and Medicine, Université de Montréal, Montreal, QC; Montreal Heart Institute Coordinating Center, Montreal, QC; and INRS-Institut Armand-Frappier, Laval, QC.

Address reprint requests to: Jocelyn Dupuis, MD, PhD, FRCP, FACC, Research Center, Montreal Heart Institute, 5000 Belanger Street, Montreal, QC H1T 1C8; e-mail: dupuisj@me.com.

DOI 10.2310/7290.2015.00003

DECKER

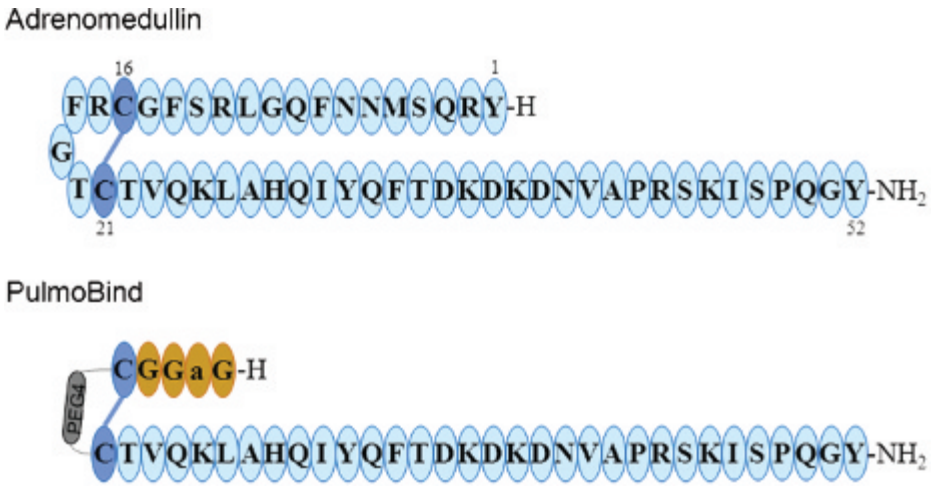

Figure S1. Amino acid sequences of human adrenomedullin and PulmoBind. The color *blue* depicts residues from the endogenous peptide sequence (human adrenomedullin), *orange* the ^{99m}Tc-chelating moiety, and *gray* the polyethylene glycol–4 spacer substituting the four intracyclic residues. The International Union of Pure and Applied Chemistry (IUPAC) one-letter code was used to identify amino acids, with uppercase and lowercase letters associated with L and D configuration, respectively.

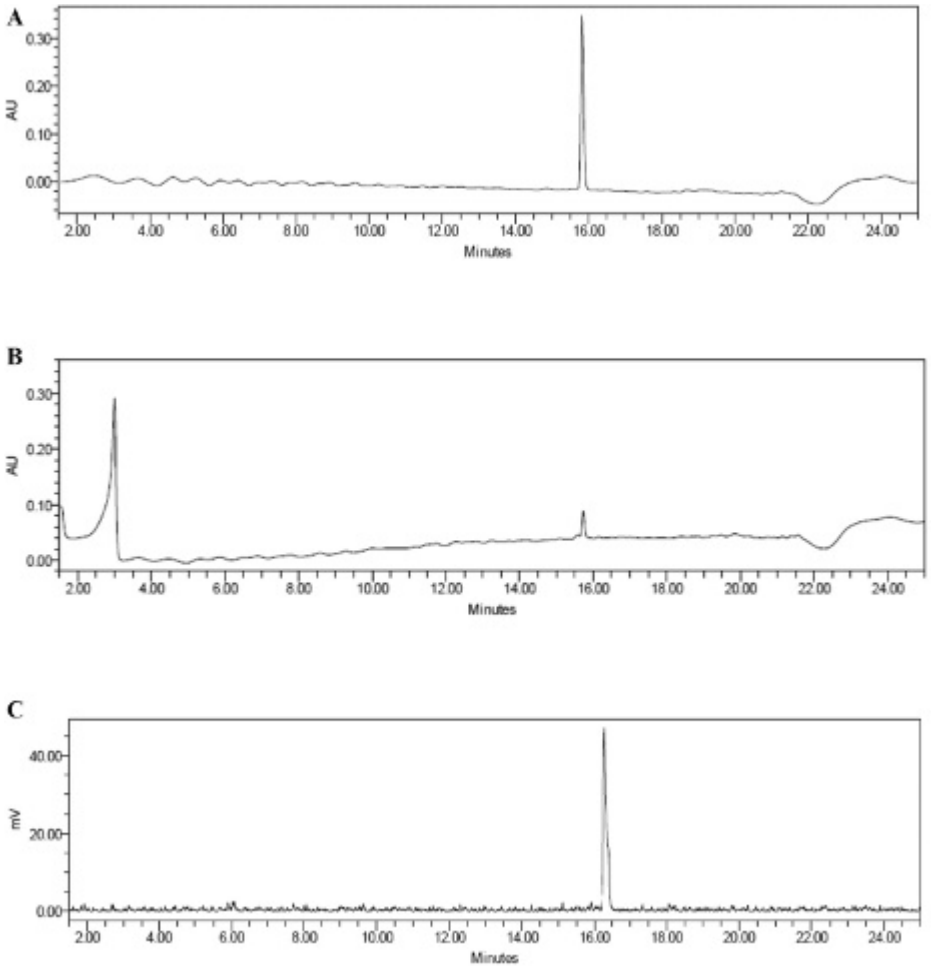

Figure S2. HPLC elution profiles of (A) PulmoBind (14.4 μM, t_R = 15.8 min) and (B) ^{99m}Tc-PulmoBind (1.44 μM) as observed with a UV detector set at 220 nm, with (C) corresponding signals collected from the radiometric detector mounted to the UV detector outlet. For each analysis, 20 μL was injected onto a C_{18} Waters X-Bridge BEH column (3.5 μm, 3.0 × 150 mm) connected to a system composed of 2 Waters 501 Pumps, a Waters 2707 autosampler, a Waters 2998 Photodiode Array (PDA) detector, and an Eckert & Ziegler Flow Count Base Fc-1000 radiometric detector. Elution was achieved by a linear gradient from 3 to 40% acetonitrile in water containing 0.1% trifluoroacetic acid.

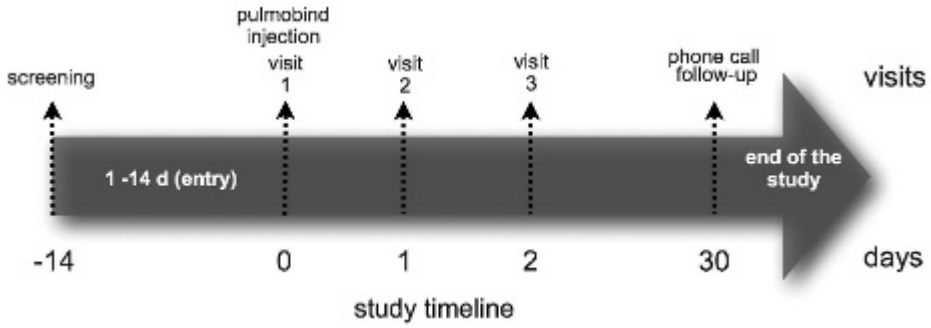

Figure S3. Study timeline.

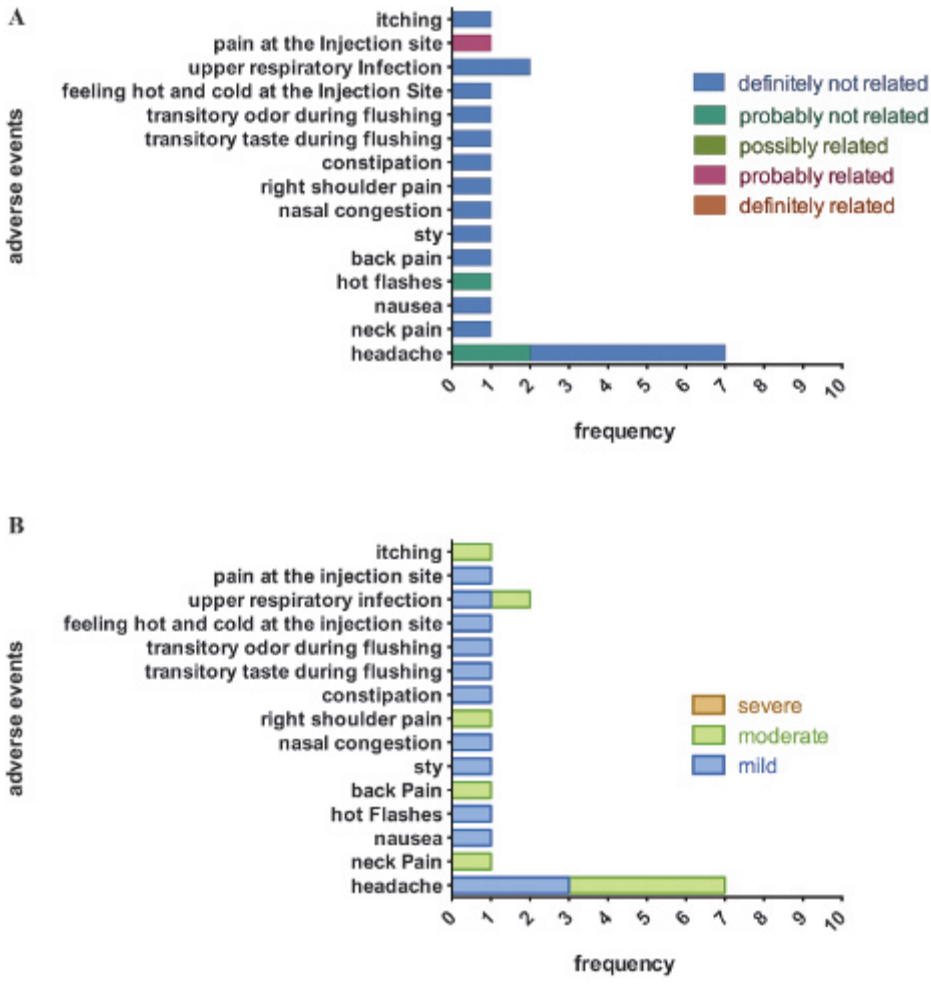

Figure S4. Study adverse events. *Top figure:* Frequency of adverse events and relationship to PulmoBind. *Bottom figure:* Frequency of adverse events and intensity.

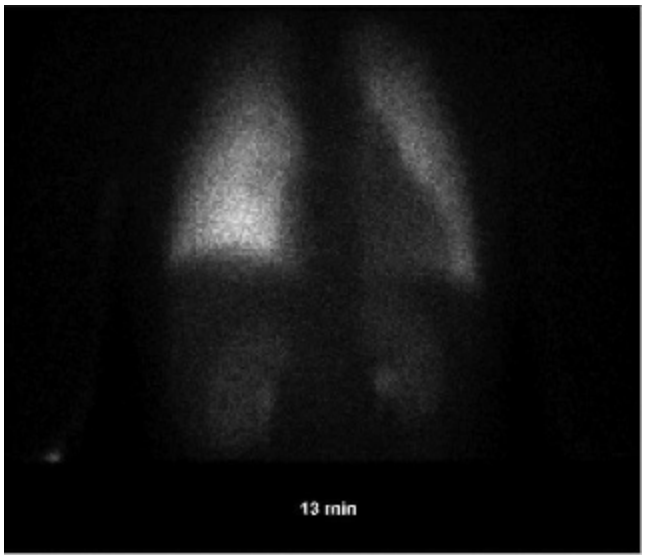

Video S1. Dynamic uptake of ^{99m}Tc-PulmoBind in humans over 6 hours following intravenous injection.

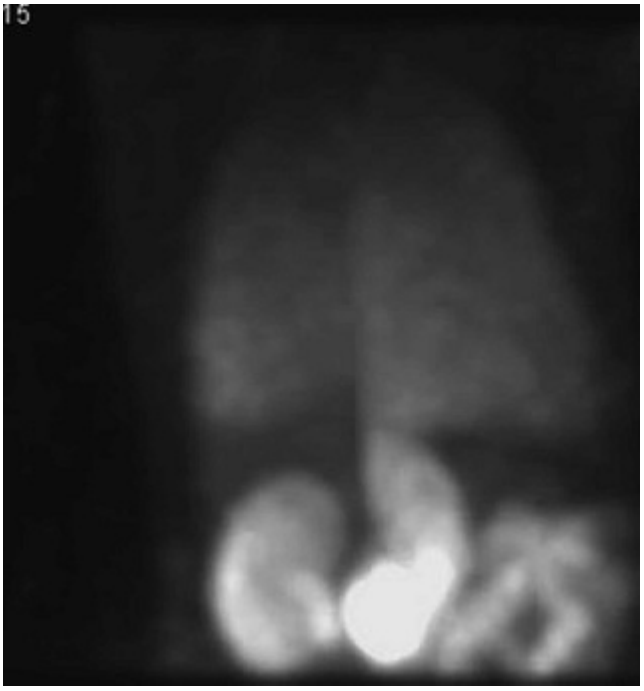

Video S2. Tomographic reconstruction of lung imaging with ^{99m}Tc-PulmoBind 90 minutes after injection.